



Get Clarity On Generics

Cost-Effective CT & MRI Contrast Agents

 **FRESENIUS
KABI**

[WATCH VIDEO](#)

AJNR

This information is current as
of August 10, 2025.

Quantitative Estimation of Permeability Surface-Area Product in Astroglial Brain Tumors Using Perfusion CT and Correlation with Histopathologic Grade

R. Jain, S.K. Ellika, L. Scarpace, L.R. Schultz, J.P. Rock, J.
Gutierrez, S.C. Patel, J. Ewing and T. Mikkelsen

AJNR Am J Neuroradiol 2008, 29 (4) 694-700

doi: <https://doi.org/10.3174/ajnr.A0899>

<http://www.ajnr.org/content/29/4/694>

ORIGINAL RESEARCH

R. Jain
S.K. Ellika
L. Scarpace
L.R. Schultz
J.P. Rock
J. Gutierrez
S.C. Patel
J. Ewing
T. Mikkelsen



Quantitative Estimation of Permeability Surface-Area Product in Astroglial Brain Tumors Using Perfusion CT and Correlation with Histopathologic Grade

BACKGROUND AND PURPOSE: Glioma angiogenesis and its different hemodynamic features, which can be evaluated by using perfusion CT (PCT) imaging of the brain, have been correlated with the grade and the aggressiveness of gliomas. Our hypothesis was that quantitative estimation of permeability surface area product (PS), cerebral blood volume (CBV), cerebral blood flow (CBF), and mean transit time (MTT) in astroglial brain tumors by using PCT will correlate with glioma grade. High-grade gliomas will show higher PS and CBV as compared with low-grade gliomas.

MATERIALS AND METHODS: PCT was performed in 32 patients with previously untreated astroglial tumors (24 high-grade gliomas and 8 low-grade gliomas) by using a total acquisition time of 170 seconds. World Health Organization (WHO) glioma grades were compared with PCT parameter absolute values by using Student or nonparametric Wilcoxon 2-sample tests. Receiver operating characteristic (ROC) analyses were also done for each of the parameters.

RESULTS: The differences in PS, CBV, and CBF between the low- and high-grade tumor groups were statistically significant, with the low-grade group showing lower mean values than the high-grade group. ROC analyses showed that both CBV (C-statistic 0.930) and PS (C-statistic 0.927) were very similar to each other in differentiating low- and high-grade gliomas and had higher predictability compared with CBF and MTT. Within the high-grade group, differentiation of WHO grade III and IV gliomas was also possible by using PCT parameters, and PS showed the highest C-statistic value (0.926) for the ROC analyses in this regard.

CONCLUSIONS: Both PS and CBV showed strong association with glioma grading, high-grade gliomas showing higher PS and CBV as compared with low-grade gliomas. Perfusion parameters, especially PS, can also be used to differentiate WHO grade III from grade IV in the high-grade tumor group.

Quantifying tumor neoangiogenesis and neovascularity is important in predicting tumor grade, treatment options, treatment response, and prognosis because it appears to play a central role in the growth and spread of tumors. However, it has been difficult to assess tumor angiogenesis primarily because of the complexity of the microvascular environment of the tumors as well as because of limited resolution of the available clinical imaging tools. Microvascular density has been used as the gold standard to assess this because of its direct association with angiogenic growth factor expression, tumor growth, and occurrence of metastases.^{1,2} Increased vascular permeability has also been associated with malignant tumor microvessels and has been evolving as a surrogate marker of tumor angiogenesis and thus tumor grade.³ Higher permeability has been associated with higher tumor grade⁴⁻⁸ and has also been shown to decrease in response to antiangiogenic therapy due to decreased tumor growth predicting tumor response.⁹ Noninvasive measurement of vascular permeability has been done by using various MR perfusion techniques, which also have been correlated with glioma grading and

treatment response.^{6,7,10-13} Perfusion CT (PCT) has been used for assessment of brain tumors¹⁴⁻¹⁷ and has a number of advantages over MR imaging techniques, the most important of which may be the linearity of signal-intensity change to tissue concentration of contrast agent, which may not be the case with MR perfusion.¹⁸⁻²¹ With PCT, multiple perfusion parameters such as permeability surface-area product (PS), cerebral blood volume (CBV), cerebral blood flow (CBF), and mean transit time (MTT) can be obtained with a single acquisition, which may be difficult with a single MR perfusion technique. Hence, in the present study, PCT was used to measure PS, CBV, CBF, and MTT in 32 patients with previously untreated gliomas; we hypothesized that glioma grade would be correlated with various perfusion parameters and high-grade gliomas would show higher PS and CBV as compared with low-grade gliomas.

Materials and Methods

Patient Population

Our Health Insurance Portability and Accountability Act-compliant study was approved by the institutional review board, and an informed consent was obtained from each participant before the study. Between January 2006 and February 2007, 40 patients with previously untreated or treatment-naïve gliomas underwent PCT. Eight patients with oligodendrogliomas were excluded from this analysis because oligodendrogliomas are known to have higher blood volume as compared with the astroglial tumors.²² Of 32 patients included in this study, 8 patients had low-grade gliomas (World Health Organization

Received August 10, 2007; accepted after revision October 17.

From the Division of Neuroradiology, Departments of Radiology (R.J., S.K.E., S.C.P.), Neurosurgery (L.S., J.P.R., T.M.), Biostatistics and Research Epidemiology (L.R.S.), Pathology (J.G.), and Neurology (J.E.), Henry Ford Hospital, Detroit, Mich.

Please address correspondence to Rajan Jain, MD, Division of Neuroradiology, Department of Radiology, Henry Ford Health System, 2799 West Grand Blvd, Detroit MI 48202; e-mail: rajanj@rad.hfh.edu

 Indicates article with supplemental on-line table.

DOI 10.3174/ajnr.A0899

[WHO] grades I and II) and 24 patients had high-grade gliomas (WHO grades III and IV). In the high-grade group, 18 patients had glioblastoma multiforme and 6 patients had anaplastic astrocytomas (On-line Table). Twenty-seven patients underwent cytoreductive surgery (subtotal resection, 25; gross total resection, 2), and 5 patients had biopsies obtained from the tumor. All the histopathologic specimens were examined by a board-certified pathologist (J.G.) and were graded as per WHO guidelines. Ages of the patients ranged from 25 to 70 years (mean, 47.78 years), and there were 20 men and 12 women. All patients underwent PCT before any treatment except 13 patients who were on a stable dose of corticosteroids at the time of PCT examination. Tumor contrast enhancement was recorded on preoperative MR imaging for all patients (On-line Table). Tumor area was also measured on postcontrast T1-weighted images on the axial section showing the largest tumor dimensions and ranged from 4.24 to 35.37 cm² (mean, 14.35 cm²).

Perfusion CT Technique

Perfusion studies were performed by using 16-section (LightSpeed; GE Healthcare, Milwaukee, Wis) and 64-section (VCT, GE Healthcare) multidetector-row CT scanners in 11 and 21 patients, respectively. A non-contrast CT head study was done to localize the region of interest before obtaining a perfusion scan. For the perfusion scan, 50 mL of nonionic contrast (ioversol; Optiray 300 mg/mL, Mallinckrodt, St. Louis, Mo) was injected at a rate of 4 mL/s through a 20-gauge intravenous line by using an automatic power injector. At 5 seconds into the injection, a cine (continuous) scanning was initiated with the following technique: 80 kVp, 190–200 mA, and 1 second per rotation for a duration of 50 seconds. After the initial 50-second cine scanning, 8 more axial images were acquired, 1 image every 15 seconds for an additional 2 minutes, thus giving a total acquisition time of 170 seconds. Four 5-mm-thick axial sections were acquired with the 16-section CT scanner, which were reformatted into two 10-mm-thick sections, whereas for the 64-section CT scanner, eight 5-mm-thick axial sections were acquired, resulting in a total coverage area of 4 cm instead of 2 cm with the 16-section scanner. Perfusion maps of CBV, CBF, MTT, and PS were generated at an Advantage Windows workstation by using CT perfusion 3.0 software (GE Healthcare) and a 2-compartment model in all patients. We used the superior sagittal sinus as the venous output function in all patients and the artery with the greatest peak and slope on time-attenuation curves as the arterial input function. A region of interest was drawn within the confines of a large vessel, and the automatic function of the software picked the pixels with the greatest peak and slope on the time-attenuation curve for analysis. The anterior cerebral artery was used as the arterial input function for the generation of perfusion maps in 28 patients, the middle cerebral artery was used in 3 patients, and the basilar artery was used in 1 patient.

Permeability Surface-Area Product (PS)

PS characterizes the diffusion of some of the contrast agent from the blood vessels into the interstitial space due to deficient or leaky blood-brain barrier (BBB). Permeability is related to the diffusion coefficient

of the contrast agent in the assumed water-filled pores of the capillary endothelium. The diffusion flux of contrast agent across the capillary endothelium is dependent on both the diffusion coefficient and the total surface area of the pores. PS is computed from the impulse residue function (IRF). Contrast agent diffusion appears in the IRF as a residual enhancement that occurs after the initial impulse response and that decreases exponentially with time. The IRF is used to estimate the first-pass fraction of contrast agent that remains in the tissue, the extraction fraction, E .²³ The extraction fraction is related to the rate at which contrast leaks out of the vasculature via the following relationship:

$$E = 1 - e^{-\frac{PS}{F}},$$

where PS is the permeability surface-area product and F is flow. The PS product has the same dimensions as flow, and thus the ratio $\frac{PS}{F}$ is dimensionless. In physiologic terms, PS is the rate at which contrast agent flows into the extravascular tissues; it is related to another commonly stated parameter of vascular leakage, the transfer constant by, the following:

$$K^{trans} = EF,$$

where K^{trans} is the transfer constant with, again, the same dimensions as flow. It is easily demonstrated that if $\frac{PS}{F} < 1$, then $K^{trans} \approx PS$. In normal cerebral vasculature, PS is negligible for all contrast agents presently in use.

Perfusion CT Map Analysis

Regions of interest were drawn on the PCT maps by 2 authors (R.J., S.K.E.) by consensus in all cases. MR images obtained before the PCT examination were evaluated for the size and the extent of the tumor on the basis of enhancing or nonenhancing solid and necrotic/cystic parts, and this observation was used to help guide drawing the regions of interest on PCT maps. Regions of interest were manually drawn to include the solid portions of the tumor, taking care not to include necrotic/cystic parts of the tumor, especially in higher grade tumors, and also by avoiding any major cortical vessels on each axial CT section. Absolute values and SDs of various perfusion parameters, such as PS (milliliters per 100 grams per minute), CBV (milliliters per 100 grams), CBF (milliliters per 100 grams per minute), and MTT (seconds) within the tumoral region of interest were recorded. We obtained means of these parameters from all the regions of interest placed on each CT section, trying to cover as much of the tumor as possible (ie, 2-cm coverage with the 16-section CT scanner and 4-cm coverage with the 64-section CT scanner).

Statistical Analysis

Descriptive statistics (means and SDs) for each parameter were computed for the different tumor groups. The tumor groups were compared by using Student or nonparametric Wilcoxon 2-sample tests. In addition, receiver operating characteristic (ROC) analyses were done

Table 1: Perfusion parameters and ROC analysis for low- and high-grade gliomas

Group (No. of patients)	PS (mL/100 g/min) Mean (SD)	CBV (mL/100 g) Mean (SD)	CBF (mL/100 g/min) Mean (SD)	MTT (s) Mean (SD)
Low grade (8)	0.52 (0.15)	0.95 (0.22)	27.0 (8.3)	4.24 (1.42)
High grade (24)	2.37 (1.40)	2.79 (1.20)	82.0 (73.7)	4.67 (1.37)
<i>P</i> value	<.001	<.001	.0024	.564
C-statistic	0.927	0.930	0.849	0.573

ROC indicates receiver operating characteristic; PS, permeability surface-area product; CBV, cerebral blood volume; CBF, cerebral blood flow; MTT, mean transit time.

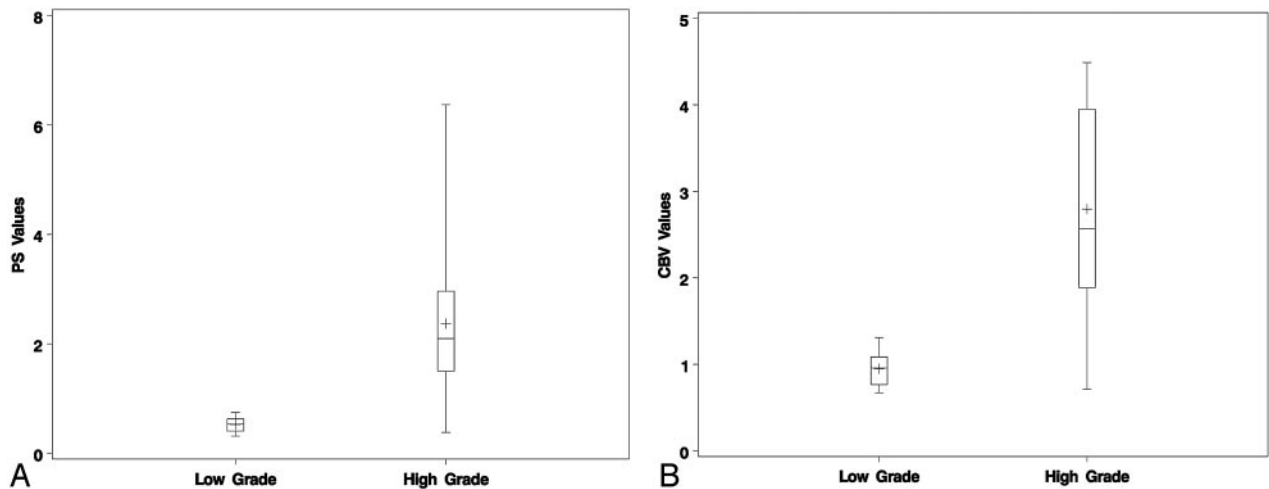


Fig 1. Box and whisker graph showing PS (A) and CBV (B) for low-versus-high-grade astroglial tumors.

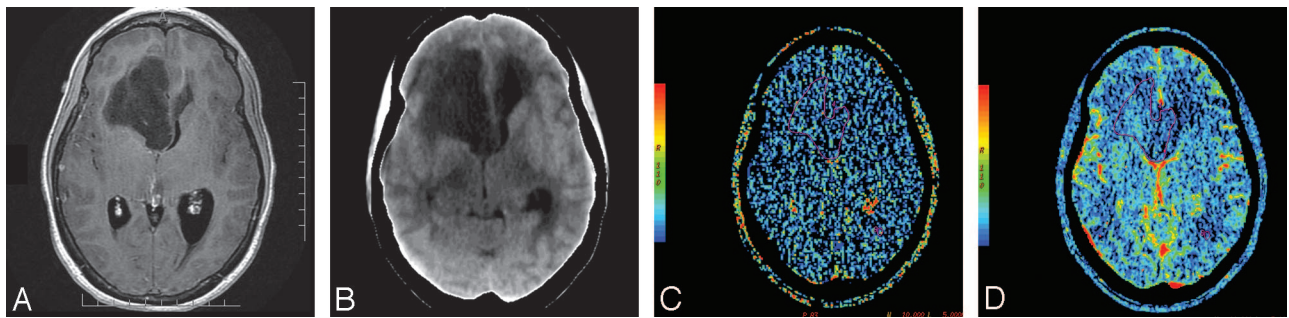


Fig 2. A and B, Postcontrast T1-weighted (TR/TE, 3059/6.35 ms) axial image (A) and base image from perfusion CT study (B) in 32-year-old woman with WHO grade II astrocytoma showing a nonenhancing right frontal tumor with no surrounding perilesional edema. C and D, PS (C) and CBV (D) perfusion CT maps showing low permeability (PS = 0.7 mL/100 g per minute) and low blood volume (CBV = 1.01 mL/100 g) within the tumor.

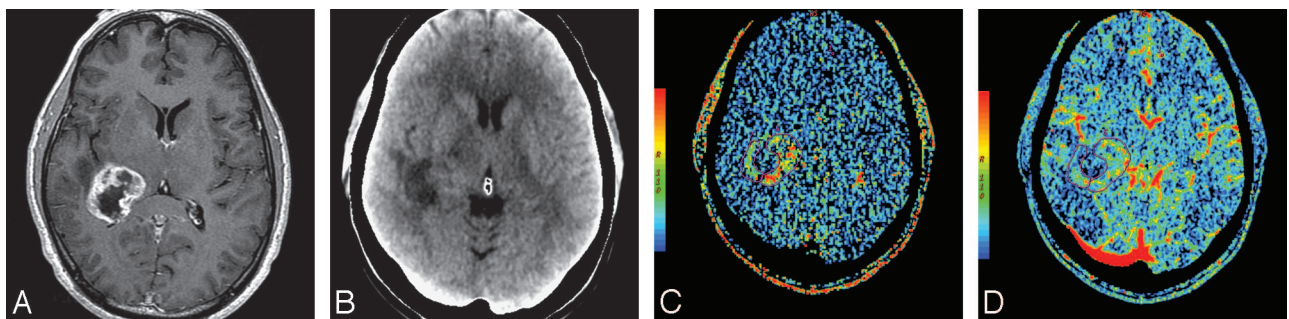


Fig 3. A, Postcontrast T1-weighted (TR/TE, 3218/5.71 ms) axial image in a 55-year-old man with glioblastoma multiforme showing a heterogeneously enhancing mass with irregular central necrosis in the right peritrigonal region. B, Base image from the perfusion CT study showing the tumor in the right peritrigonal region. C, Perfusion CT PS maps (C) showing very high permeability (PS = 5.14 mL/100 g per minute) along the enhancing nodular margins of the tumor and CBV maps (D) showing high blood volume (CBV = 3.49 mL/100 g) within the enhancing periphery of the tumor.

to compute the area under the curve (C-statistic) for each of the parameters. This statistic can help assess which parameter is the best in differentiating between different grades of glioma; the higher the C-statistic, the better is the predictability of the parameter.

Results

Low-Grade Versus High-Grade Gliomas

Table 1 contains the results for the 2 groups (Fig 1). The differences in PS, CBV, and CBF between the 2 groups were statistically significant, with the low-grade tumor group showing a lower mean value for all parameters than the high-grade group (Figs 2

and 3). However, the difference in MTT between the 2 groups was not statistically significant. ROC analyses showed that both CBV (C-statistic 0.930) and PS (C-statistic 0.927) were very similar to each other in differentiating low- and high-grade gliomas and had higher predictability compared with CBF (C-statistic 0.849) and MTT (C-statistic 0.573).

Grade III Versus Grade IV Gliomas

Within the high-grade group differentiation into grade III and grade IV gliomas also could be done by using the perfusion parameters. PS showed the highest C-statistic value (0.926) for the

Table 2: Perfusion parameters and ROC analysis for WHO grades III and grade IV

Group (No. of patients)	PS (mL/100 g/min) Mean (SD)	CBV (mL/100 g) Mean (SD)	CBF (mL/100 g/min) Mean (SD)	MTT (s) Mean (SD)
WHO grade III (6)	1.04 (0.73)	1.82 (1.41)	38.9 (19.3)	4.60 (1.62)
WHO grade IV (18)	2.81 (1.28)	3.12 (0.97)	96.3 (79.8)	4.69 (1.32)
<i>P</i> value	<.001	.039	.014	.922
C-statistic	0.926	0.787	0.833	0.509

ROC indicates receiver operating characteristic; PS, permeability surface-area product; CBV, cerebral blood volume; CBF, cerebral blood flow; MTT, mean transit time.

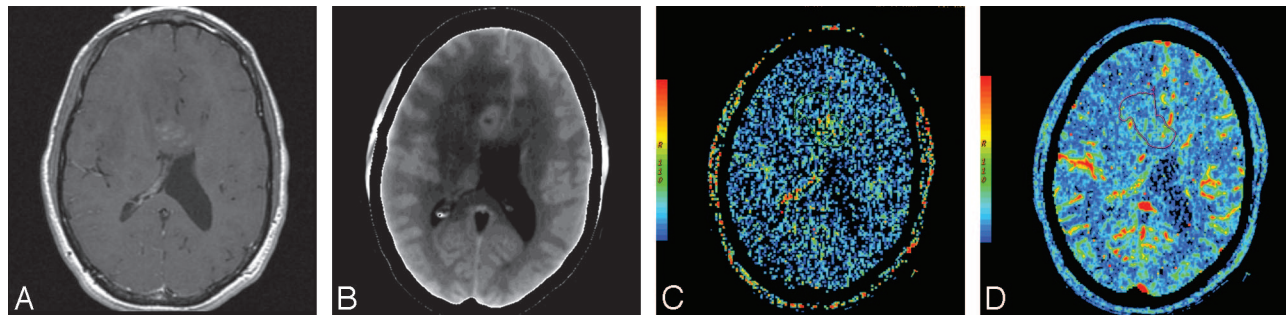


Fig 4. A and B, Postcontrast T1-weighted (TR/TE, 650/13 ms) axial image (A) and base image from perfusion CT study (B) in a 46-year-old man with a heterogeneously enhancing mass lesion predominantly involving the right frontal lobe with extension across the genu of the corpus callosum. C and D, Perfusion CT PS (C) and CBV (D) maps showing high permeability (PS = 2.04 mL/100 g per minute) and tumor blood volume (CBV = 2.21 mL/100 g). Histopathology revealed a grade III anaplastic astrocytoma.

Table 3: Perfusion parameters and *P* values for nonenhancing versus enhancing grade III, nonenhancing grade III versus low grade, and enhancing grade III versus grade IV gliomas

	PS (mL/100 g/min) Mean (SD)	CBV (mL/100 g) Mean (SD)	CBF (mL/100 g/min) Mean (SD)	MTT (s) Mean (SD)
Low grade (8)	0.52 (0.15)	0.95 (0.22)	27.0 (8.3)	4.24 (1.42)
Nonenhancing grade III (3)	0.46 (0.13)	0.88 (0.16)	26.1 (3.4)	3.23 (0.64)
Enhancing grade III (3)	1.61 (0.57)	2.77 (1.52)	51.7 (20.8)	5.96 (0.75)
WHO grade IV (18)	2.81 (1.28)	3.12 (0.97)	96.3 (79.8)	4.69 (1.32)
<i>P</i> values for nonenhancing vs. enhancing grade III	.011	.029	.055	.012
<i>P</i> values for low grade vs. nonenhancing grade III	.623	.699	.971	.330
<i>P</i> values for enhancing grade III vs. grade IV	.052	.438	.322	.128

PS indicates permeability surface-area product; CBV, cerebral blood volume; CBF, cerebral blood flow; MTT, mean transit time.

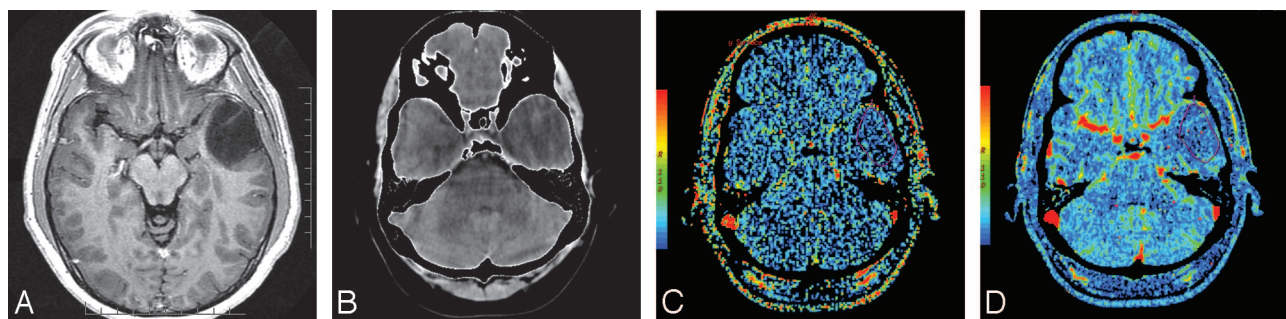


Fig 5. A and B, Postcontrast T1-weighted (TR/TE, 3103/6.35 ms) image (A) and base image from perfusion CT study (B) in a 31-year-old man who presented with memory impairment and speech problems showing a nonenhancing mass in the left temporal lobe with minimal mass effect and perilesional edema. C and D, PS (C) and CBV (D) maps showing low permeability (PSA = 0.61 mL/100 g per minute) and low blood volume (CBV = 0.92 mL/100 g) within the mass. Histopathology revealed grade III anaplastic astrocytoma.

ROC analyses, suggesting the highest predictability in differentiating grade III from grade IV as compared with other parameters (Table 2).

Nonenhancing Versus Enhancing Grade III, Nonenhancing Grade III Versus Low Grade, and Enhancing Grade III Versus Grade IV Gliomas

Out of 6 grade III gliomas, images of 3 patients showed contrast enhancement on MR imaging, and those of 3 patients did not show any contrast enhancement. Enhancing grade III gli-

omas (Fig 4 and Table 3) had a higher mean PS (1.61 versus 0.46; *P* value, .011), mean CBV (2.77 versus 0.88; *P* value, .029), mean CBF (51.7 versus 26.1; *P* value, .055), and also a higher mean MTT (5.96 versus 3.23; *P* value, .012) as compared with nonenhancing grade III gliomas (Fig 5 and Table 3). However, no statistically significant differences were seen as far as differentiating low-grade gliomas, none of which showed any contrast enhancement (On-line Table), from nonenhancing grade III gliomas on the basis of PCT parameters. Similarly in differentiating enhancing grade III from

grade IV gliomas, all of which showed contrast enhancement, only PS showed borderline statistical significance (P value, .052), and the rest of the perfusion parameters did not show any statistically significant difference (Table 3).

Discussion

Tumor Vascular Permeability: Common Facts and Their Importance

It is a common fact that tumor blood vessels have defective and leaky endothelium. Hypoxia or hypoglycemia that occurs in rapidly growing tumors increases the expression of vascular endothelial growth factor (VEGF), which is not only a potent angiogenic factor but also a potent permeability factor.^{24,25} VEGF leads to the development of neoangiogenic vessels, which are immature and tortuous^{26,27} and also have increased permeability to macromolecules due to large endothelial cell gaps, incomplete basement membrane, and absent smooth muscle.²⁸ These abnormal tumor vessels can be used as potential markers to assess the tumor grade. Grading of gliomas is important from the perspective of treatment and patient prognosis. The current standard for tumor grading is histopathologic assessment of tissue, which has inherent limitations, such as sampling error, interobserver variation, and a wide variety of classification systems that are available, of which the most commonly used is the WHO grading system.^{29,30} Thus in vivo measurement of tumor-vessel permeability is important for various reasons: 1) It can be used for grading of tumors because increased permeability is associated with immature blood vessels, which is seen with neoangiogenesis; 2) it can be used to study the response of tumors to various therapies, especially antiangiogenic therapy³¹; 3) understanding the concept of permeability can help in understanding the mechanism of entry of therapeutic agents into the central nervous system; and 4) it can be used for development of methods to alter selectively the BBB to enhance drug delivery.³²

In Vivo Permeability Measurement: Imaging Techniques, Limitations, and Controversies

Various noninvasive imaging techniques have been increasingly used to characterize and grade brain tumors because histologic tumor grade alone can be an unreliable predictor of patient outcome and there is a shift in the role of imaging to provide physiologic information in addition to morphologic characteristics. Perfusion imaging can provide information about flow dynamics of tumor vessels, particularly blood volume and permeability measurements that can be complementary to conventional imaging for preoperative grading of gliomas,^{6,33-35} and can also help us understand biologic differences between tumors of the same grade and response of tumors to therapy. MR and CT perfusion have been used for in vivo characterization of tumor angiogenesis in various animal and human studies.³⁶⁻⁴⁰

One of the major limitations of clinically used imaging techniques has been low spatial resolution, which limits assessment of the complex and heterogeneous vascular microenvironment in detail.^{41,42} Another limitation has been the current use of low-molecular-weight contrast agents for human subjects. Because permeability measurements depend on the leakage of particles from the blood to the interstitial space, it is hypothesized that low-molecular-weight contrast agents

leak relatively easily from the blood into the interstitium. This might also lead to overestimation of the permeability, which will be influenced by and will approximate tumor blood flow.⁴³ High-molecular-weight contrast agents leak from the vessels and move through the interstitium with relative difficulty and are flow-independent. Thus macromolecular permeability and vascular volumes may be best measured by high-molecular-weight contrast agents.⁴³ However, currently used CT or MR imaging contrast agents are of low molecular weight (~ 0.5 – 0.9 kDa), which might limit the accurate differentiation of vascular permeability and blood volume.⁴⁴ Even though CT and MR imaging contrast agents do not differ much in their molecular weight, different charges of nonionic CT contrast as compared with ionic MR imaging contrast may also be responsible for the differences in permeability measured with these 2 modalities.

Another controversial aspect of measuring permeability with various perfusion imaging techniques has been the scanning time. Delayed permeability due to slow leakage of contrast from a leaky blood vessel may not be accurately measured with the first pass of the contrast agent by using a 45- or 60-second scanning time^{10,45} and can be measured only with longer acquisition times; however, there is no real consensus about the optimal acquisition time. The permeability values we obtained are higher than the values reported in the literature, and this could be explained by the mathematic model that is used with PCT. In the present study, the acquisition time of 170 seconds could also explain the higher values that we obtained because this scanning sequence was optimized to include delayed permeability as also described previously. Gliomas, particularly high-grade gliomas, can have extremely variable and heterogeneous blood flow due to the complex tumor vasculature, which can influence permeability.^{42,43,46} Other factors that can also influence permeability include luminal surface area and interstitial, hydrostatic, and osmotic pressure across the endothelium. Slow blood flow or low osmotic gradients, which can occur in high-grade tumor with a lot of vasogenic edema and also in the central parts of large tumors, can lead to a larger component of delayed permeability, requiring longer acquisition times. In the present study, we used an acquisition time of 170 seconds to measure delayed permeability.

Quantification of vessel permeability with various perfusion techniques requires 2 or more compartment pharmacokinetic models with an arterial input function, making these studies more complex than CBV estimation,⁴⁷ and is dependent on the imaging technique and the mathematic model used. Postgadolinium T1-weighted MR imaging gives a rough estimate of the disruption of the BBB and has been used in the past for quantitative estimation of permeability, but dynamic imaging acquisition provides a better estimate of vascular permeability.⁴⁷ Dual-echo gradient-echo perfusion-weighted imaging⁴⁸ is based on a simple 2-compartment kinetic model⁴⁹ and has more recently been used to measure vascular permeability and to estimate correctly blood volume in brain tumors with deficient or absent BBB. There are several studies that have found a correlation between increased vascular permeability and higher tumor grade.^{6,10,33-35} However, MR perfusion techniques have certain limitations because of the nonlinear relationship of the signal intensity with the contrast, both for dynamic contrast-enhanced imaging with T1-weighting^{18-20,50} and for dynamic susceptibility contrast imaging

with T2- or T2*-weighting. In the latter case, if the contrast agent remains intravascular, the method is widely accepted as a relative estimate of CBF and CBV, though there is a possibility for artifacts because of difficulties in assessing the shape and timing of the arterial input function.⁵¹⁻⁵⁷

In the event that substantial leakage of contrast agent from intra- to extravascular space takes place, a strong and competing T1 contrast effect is often noticed in areas of pathology because of the necessity of short (approximately 1 second) repetition times needed to estimate CBF. As a first-order tactic to minimize the competing T1 contrast, preloading with contrast agent has been proposed,⁴⁹ with some success. However, this approach does not allow an estimate of K^{trans} . An alternative has also been proposed.⁵⁸ To decrease the T1 effect, this approach used a slower TR, lengthening the TR of the experiment and undermining the estimation of CBF, thus yielding only estimates of CBV and K^{trans} . A further refinement, allowing the estimate of blood volume and producing an index of transfer constant, has been suggested,⁴⁹ and a dual-echo gradient-echo sequence⁴⁸ also shows some potential for an index of blood volume and transfer constant. Despite the partial success of these rapid imaging studies, in contrast to CT perfusion, there does not appear to be an MR imaging technique that will reliably quantify CBF, CBV, and K^{trans} in 1 experiment. Another major disadvantage of MR perfusion is susceptibility artifacts due to hemorrhage and various mineral depositions, which can be a major issue in posttreatment tumor patients.

Relationship Between Glioma Grade and Perfusion CT Parameters

In the present study, we could differentiate the high-grade tumor group into grade III and grade IV on the basis of perfusion parameters (Table 2), and especially PS showed a stronger association (P value < .001) with glioma grade than CBV, CBF, or MTT. This is in keeping with the current WHO guidelines of including microvascular proliferation as a diagnostic criterion of grade IV but not for grade III astrocytic tumors. Increased angiogenesis in grade IV tumors is characterized by an increased number and density of vessels as compared with grade III astrocytic tumors.⁵⁹ Grade IV tumor vessels are especially characterized by disproportionate lengthening, increased pliability, and irregular shape,⁵⁹ which can explain the difference in perfusion parameters for grade IV as compared with grade III tumors.

Within the WHO grade III group, 3 patients had nonenhancing infiltrative tumors, whereas 3 patients showed contrast enhancement on MR imaging. Nonenhancing grade III tumors showed lower mean PS, CBV, and CBF as compared with the enhancing grade III group (Table 3). This difference is probably due to more microvascular density and proliferation seen in enhancing tumors as compared with the nonenhancing group. This could have prognostic implications because the enhancing grade III tumors that show higher PS, CBV, and CBF may be more aggressive, with a higher recurrence rate and shorter survival periods as compared with the nonenhancing grade III, which remains to be determined. The present study is limited because the number of patients in these 2 subgroups is small, and it also does not have survival or follow-up data.

It is possible to underestimate the grade of nonenhancing tumors solely on the basis of morphologic imaging features. The perfusion parameters, which are primarily based on esti-

mation of microvascular proliferation and tumor neoangiogenesis, also may not help in such a scenario. In the present study, we did not find any statistically significant difference of any of the perfusion parameters for differentiating nonenhancing grade III gliomas from low-grade gliomas (WHO grades I and II), all of which did not show any contrast enhancement. This could be explained by the fact that the only difference between these groups was presence or absence of mitosis by WHO grading criteria, and most of these nonenhancing grade III gliomas showed very little microvascular proliferation. For differentiating enhancing grade III gliomas from grade IV, only PS showed a borderline statistical significance; however, the present analysis is also limited by the small number of enhancing grade III gliomas. This potential role of PS in differentiating these 2 groups is probably based on the difference and complexity of angioarchitecture.⁵⁹

Limitations of the Study

Limitations of the study include: 1) a relatively small sample size, 2) questionable reproducibility of absolute perfusion CT parameters by using different arterial input and venous output functions, 3) surgical sampling error could be another potential limitation particularly in cases in which the histologic specimen was obtained with biopsy only, and 4) steroids can also influence the perfusion parameters, particularly PS, and only 13 out of 32 patients in the present study were on a stable dose of corticosteroids at the time of PCT examination.

Conclusions

Perfusion CT can be used with a longer acquisition time to measure PS, including delayed permeability in gliomas. Both PS and CBV have shown strong association with glioma grading. These 2 perfusion parameters may be measuring 2 slightly different aspects of tumor microvasculature and may also provide different information about tumor biology. Further long-term and larger studies will be required to investigate which perfusion parameter correlates better with treatment outcome and prognosis. Perfusion parameters can also be used to differentiate grade III from grade IV in the high-grade tumor group, with PS showing slightly stronger association as compared with CBV and CBF in the present study. CT perfusion parameters provide physiologic information, which may supplement conventional morphologic imaging in predicting glioma grade and may also be useful in assessing response to various therapies in the future.

References

1. Phongkitkarun S, Kobayashi S, Kan Z, et al. Quantification of angiogenesis by functional computed tomography in Matrigel model in rats. *Acad Radiol* 2004;11:573-82
2. Weidner N. Intratumor microvessel density as a prognostic factor in cancer. *Am J Pathol* 1995;147:9-19
3. van Dijke CF, Brasch RC, Roberts TP, et al. Mammary carcinoma model: correlation of macromolecular contrast-enhanced MR imaging characterizations of tumor microvasculature and histologic capillary density. *Radiology* 1996;198:813-18
4. Gossmann A, Okuhata Y, Shames DM, et al. Prostate cancer tumor grade differentiation by dynamic contrast-enhanced MR imaging in the cat: comparison of macromolecular and small-molecular contrast media—preliminary experience. *Radiology* 1999;213:265-72
5. Daldrop H, Shames DM, Wendland M, et al. Correlation of dynamic contrast-enhanced MR imaging with histologic tumor grade: comparison of macromolecular and small-molecular contrast media. *AJR Am J Roentgenol* 1998;171:941-49
6. Roberts HC, Roberts TP, Brasch RC, et al. Quantitative measurement of mi-

- crovascular permeability in human brain tumors achieved using dynamic contrast-enhanced MR imaging: correlation with histologic grade. *AJNR Am J Neuroradiol* 2000;21:891–99
7. Roberts HC, Roberts TP, Bollen AW, et al. Correlation of microvascular permeability derived from dynamic contrast enhanced MR imaging with histologic grade and tumor labeling index: a study in human brain tumors. *Acad Radiol* 2001;8:384–91
8. Yuan F, Salehi HA, Boucher Y, et al. Vascular permeability and microcirculation of gliomas and mammary carcinomas transplanted in rat and mouse cranial windows. *Cancer Res* 1994;54:4564–68
9. Pham CD, Roberts TP, van Bruggen N, et al. Magnetic resonance imaging detects suppression of tumor vascular permeability after administration of antibody to vascular endothelial growth factor. *Cancer Invest* 1998;16:225–30
10. Law M, Yang S, Babb JS, et al. Comparison of cerebral blood volume and vascular permeability from dynamic susceptibility contrast-enhanced perfusion MR imaging with glioma grade. *AJNR Am J Neuroradiol* 2004;25:746–55
11. Law M, Oh S, Johnson G, et al. Perfusion magnetic resonance imaging predicts patient outcome as an adjunct to histopathology: a second reference standard in the surgical and nonsurgical treatment of low grade gliomas. *Neurosurgery* 2006;58:1099–107
12. Gossman A, Helbich TH, Kuriyama N, et al. Dynamic contrast-enhanced magnetic resonance imaging as a surrogate marker of tumor response to anti-angiogenic therapy in a xenograft model of glioblastoma multiforme. *J Magn Reson Imaging* 2002;15:233–40
13. Cao Y, Shen Z, Chenevert TL, et al. Estimate of vascular permeability and cerebral blood volume using Gd-DTPA contrast enhancement and dynamic T2*-weighted MRI. *J Magn Reson Imaging* 2006;24:288–96
14. Jain R, Scarpace L, Ellika SK, et al. First pass perfusion computed tomography: initial experience in differentiating recurrent tumors from radiation effects and radiation necrosis. *Neurosurgery*. 2007;61:778–86
15. Ellika SK, Jain R, Patel SC, et al. Role of perfusion CT in glioma grading and comparison with conventional MR imaging features. *AJNR Am J Neuroradiol* 2007;28:1981–87
16. Roberts HC, Roberts TP, Lee TY, et al. Dynamic, contrast-enhanced CT of human brain tumors: quantitative assessment of blood volume, blood flow, and microvascular permeability—report of two cases. *AJNR Am J Neuroradiol* 2002;23:828–32
17. Ding B, Ling HW, Chen KM, et al. Comparison of cerebral blood volume and permeability in preoperative grading of intracranial glioma using CT perfusion imaging. *Neuroradiology* 2006;48:773–81
18. Yankeelov TE, Rooney WD, Huang W, et al. Evidence for shutter-speed variation in CR bolus-tracking studies of human pathology. *NMR Biomed* 2005;18:173–85
19. Li X, Rooney WD, Springer CS. A unified magnetic resonance imaging pharmacokinetic theory: intravascular and extracellular contrast reagents. *Magn Reson Med* 2005; 54:1351–59
20. Yankeelov TE, Rooney WD, Li X, et al. Variation of the relaxographic “shutter-speed” for transcytolemmal water exchange affects the CR bolus-tracking curve shape. *Magn Reson Med* 2003;50:1151–69
21. Landis CS, Li X, Telang FW, et al. Determination of the MRI contrast agent concentration time course in vivo following bolus injection: effect of equilibrium transcytolemmal water exchange. *Magn Reson Med* 2000;44:563–74
22. Lev MH, Ozsunar Y, Henson JW, et al. Glioma tumor grading and outcome prediction using dynamic spin-echo MR susceptibility mapping compared with conventional contrast-enhanced MR: confounding effect of elevated rCBV of oligodendrogliomas. *AJNR Am J Neuroradiol* 2004;25:214–21
23. Purdie TG, Henderson E, Lee TY. Functional CT imaging of angiogenesis in rabbit VX2 soft-tissue tumor. *Phys Med Biol* 2001;46:3161–75
24. Shweiki D, Itin A, Soffer D, et al. Vascular endothelial growth factor induced by hypoxia may mediate hypoxia-initiated angiogenesis. *Nature* 1992;359:843–45
25. Plate KH, Breier G, Weich HA, et al. Vascular endothelial growth factor is a potential tumor angiogenesis factor in human gliomas in vivo. *Nature* 1992;359:845–48
26. Jain RK. Determinants of tumor blood flow: a review. *Cancer Res* 1988;48:2641–58
27. Jain RK, Munn LL, Fukumura D. Dissecting tumor pathophysiology using intravital microscopy. *Nat Rev Cancer* 2002;2:266–76
28. Hashizume H, Baluk P, Morikawa S, et al. Openings between defective endothelial cells explain tumor vessel leakiness. *Am J Pathol* 2000;156:1363–80
29. Cha S. Update on brain tumor imaging: from anatomy to physiology. *AJNR Am J Neuroradiol* 2006;27:475–87
30. Louis DN, Ohgaki H, Wiestler OD, et al. *WHO Classification of Tumors of the Central Nervous System*. Lyon, France: WHO; 2007
31. Bhujwala ZM, Artemov D, Natarajan K, et al. Reduction of vascular and permeable regions in solid tumors detected by macromolecular contrast magnetic resonance imaging after treatment with antiangiogenic agent TNP-470. *Clin Cancer Res* 2003;9:355–62
32. Provenzale JM, Mukundan S, Dewhirst M. The role of blood-brain-barrier permeability in brain tumor imaging and therapeutics. *AJR Am J Roentgenol* 2005;185:763–67
33. Lev MH, Rosen BR. Clinical applications of intracranial perfusion MR imaging. *Neuroimaging Clin N Am* 1999;9:309–31
34. Provenzale JM, Wang GR, Brenner T, et al. Comparison of permeability in high-grade and low-grade brain tumors using dynamic susceptibility contrast MR imaging. *AJR Am J Roentgenol* 2002;178:711–16
35. Jackson A, Kassner A, Annesley-Williams D, et al. Abnormalities in the recirculation phase of contrast agent bolus passage in cerebral gliomas: comparison with relative blood volume and tumor grade. *AJNR Am J Neuroradiol* 2002;23:7–14
36. Lupo JM, Cha S, Chang SM, et al. Dynamic susceptibility-weighted perfusion imaging of high-grade gliomas: characterization of spatial heterogeneity. *AJNR Am J Neuroradiol* 2005;26:1446–54
37. Cha S, Knopp EA, Johnson G, et al. Intracranial mass lesions: dynamic contrast-enhanced susceptibility-weighted echo-planar perfusion MR imaging. *Radiology* 2002;223:11–29
38. Maia AC, Malheiros SM, da Rocha AJ, et al. MR cerebral blood volume maps correlated with vascular endothelial growth factor expression and tumor grade in nonenhancing gliomas. *AJNR Am J Neuroradiol* 2005;26:777–83
39. Cenic A, Nabavi DG, Craen RA, et al. A CT method to measure hemodynamics in brain tumors: validation and application of cerebral blood flow maps. *AJNR Am J Neuroradiol* 2000;21:462–70
40. Eastwood JD, Provenzale JM. Cerebral blood flow, blood volume, and vascular permeability of cerebral glioma assessed with dynamic CT perfusion imaging. *Neuroradiology* 2003;45:373–76
41. Vajkoczy P, Menger MD. Vascular microenvironment in gliomas. *J Neurooncol* 2000;50:99–108
42. McDonald DM, Choyke PL. Imaging of angiogenesis: from microscope to clinic. *Nat Med* 2003;9:713–25
43. de Lussanet QG, Langereis S, Beets-Tan RG, et al. Dynamic contrast enhanced MR imaging kinetic parameters and molecular weight of dendritic contrast agents in tumor angiogenesis in mice. *Radiology* 2005;235:65–72
44. Choyke PL. Contrast agents for imaging tumor angiogenesis: is bigger better? *Radiology* 2005;235:1–2
45. Goh V, Halligan S, Hugill JA, et al. Quantitative colorectal cancer perfusion measurement using dynamic contrast-enhanced multidetector-row computed tomography: effect of acquisition time and implications for protocols. *J Comput Assist Tomogr* 2005;29:59–63
46. Montermini D, Winlove CP, Michel C. Effects of perfusion rate on permeability of frog and rat mesenteric microvessels to sodium fluorescein. *J Physiol* 2002;543(Pt 3):959–75
47. Tofts PS, Brix G, Buckley DL, et al. Estimating kinetic parameters from dynamic contrast-enhanced T1-weighted MRI of a diffusible tracer: standardized quantities and symbols. *J Magn Reson Imaging* 1999;10:223–32
48. Uematsu H, Maeda M. Double-echo perfusion-weighted MR imaging: basic concepts and application in brain tumors for the assessment of tumor blood volume and vascular permeability. *Eur Radiol* 2006;16:180–86
49. Boxerman JL, Schmainda KM, Weisskoff RM. Relative cerebral blood volume maps corrected for contrast agent extravasation significantly correlate with glioma tumor grade, whereas uncorrected maps do not. *AJNR Am J Neuroradiol* 2006;27:859–67
50. Landis CS, Li X, Telang FW, et al. Equilibrium transcytolemmal water-exchange kinetics in skeletal muscle in vivo. *Magn Reson Med* 1999;42:467–78
51. Akbudak E, Norberg RE, Conturo TE. Contrast-agent phase effects: an experimental system for analysis of susceptibility, concentration, and bolus input function kinetics. *Magn Reson Med* 1997;38:990–1002
52. Conturo TE, Akbudak E, Kotys MS, et al. Arterial input functions for dynamic susceptibility contrast MRI: requirements and signal options. *J Magn Reson Imaging* 2005;22:697–703
53. Akbudak E, Conturo TE. Arterial input functions from MR phase imaging. *Magn Reson Med* 1996;36:809–15
54. Conturo TE, Barker PB, Mathews VP, et al. MR imaging of cerebral perfusion by phase-angle reconstruction of bolus paramagnetic-induced frequency shifts. *Magn Reson Med* 1992;27:375–90
55. Calamante F, Gadian DG, Connelly A. Delay and dispersion effects in dynamic susceptibility contrast MRI: simulations using singular value decomposition. *Magn Reson Med* 2000;44:466–73
56. Calamante F, Gadian DG, Connelly A. Quantification of bolus-tracking MRI: improved characterization of the tissue residue function using Tikhonov regularization. *Magn Reson Med* 2003;50:1237–47
57. Calamante F, Morup M, Hansen LK. Defining a local arterial input function for perfusion MRI using independent component analysis. *Magn Reson Med* 2004;52:789–97
58. Johnson G, Wetzel SG, Cha S, et al. Measuring blood volume and vascular transfer constant from dynamic T2*-weighted contrast-enhanced MRI. *Magn Reson Med* 2004;51:961–68
59. Sharma S, Sharma MC, Gupta DK, et al. Angiogenic patterns and their quantitation in high grade astrocytic tumors. *J Neurooncol* 2006;79:19–30